34th Annual International Conference of the IEEE EMBS
San Diego, California USA, 28 August - 1 September, 2012

# An Improved FDK Algorithm using Camera Calibration Technique for Reconstruction of Misaligned CBCT System

Mengjiao Wang, Hui Ding, and Guangzhi Wang*, *Member, IEEE*

***Abstract*—Cone beam computed tomography (CBCT) is widely applied for medical and industrial use recently. But artifacts are always induced due to the misalignments of CBCT components. An improved Feldkamp-Davis-Kress (FDK) algorithm using camera calibration technique for image reconstruction of misaligned CBCT is applied here to reduce the artifacts. Simulation results show that our improved FDK algorithm can reduce the artifacts significantly compared with standard FDK algorithm in misaligned CBCT system. Through the improved FDK algorithm presented here, we can reconstruct misaligned CBCT images efficiently.**

## I. Introduction

Cone beam computed tomography (CBCT) is widely applied for medical and industrial use recently. However, the nonidealities of CBCT geometry, especially the misalignments of detector, which can cause severe artifacts, are inevitable due to errors of mechanical assembly[1]. This makes it a significant issue to improve CBCT reconstruction algorithm for reconstruction of misaligned CBCT images.

In the past few years, many efforts have been made in improving CBCT reconstruction algorithm. In previous methods, the assumption that some parameters are ideal or negligible is always applied. The complexity of these methods increases by applying indirect and complicated geometric relationship[1-3].

In this paper, an improved FDK algorithm using camera calibration technique in computer vision is presented without assuming any parameters to be ideal or known apriority. CBCT system is considered as a combination of rotation subsystem and image subsystem, which includes X-ray source and detector and is considered as a pin-hole camera here. In image subsystem, there exists an optical axis, which is the ray that perpendicular to the planar detector. As for ideal CBCT, the direct geometric relationships between two subsystems are already determined, that is, rotation axis is perpendicular to, and intersects with optical axis. And rotation axis is parallel to the column of detector. In misaligned CBCT system, the conditions mentioned above are not satisfied. We apply camera calibration technique here to calculate the misalignment, that is, the direct geometric relationship between image and rotation subsystems in misaligned CBCT. Furthermore, an improved FDK algorithm considering the misalignment is applied to reconstruct sectional image from misaligned CBCT projections.

This work was supported by the National Basic Research Program of China (973) under Grant 2011CB707701 and research foundation of Tsinghua University.

Mengjiao Wang and Hui Ding are with the Department of Biomedical Engineering, School of Medicine, Tsinghua University, Beijing 100084, China.

*Guangzhi Wang is with the Department of Biomedical Engineering, School of Medicine, Tsinghua University, Beijing 100084, China (e-mail: wgz-dea@tsinghua.edu.cn).

## II. Methods

In this part, firstly, the concepts of standard and our improved FDK algorithm are addressed briefly. Then, the details of our improved FDK algorithm are demonstrated.

### A. Standard FDK Algorithm

FDK algorithm is widely used for CBCT reconstruction. The standard FDK algorithm consists of four steps[4]:

(1) calculating the projection coordinate of the constructed voxel on the detector

(2) weighting of raw, acquired projections

(3) filtering of weighted projections

(4) cone-beam backprojection of weighted and filtered projections

### B. Improved FDK Algorithm

In our improved FDK algorithm, two parts was changed. One was the projection coordinate of the reconstructed voxel on the misaligned detector. The other one was the weighting factor based on the reconstructed voxel. The filtering and backprojection procedures were the same to the standard algorithm.

To apply our improved FDK algorithm, three steps were taken:

(1) For calculation of the two changed parts, firstly, camera calibration technique was applied to obtain the internal and external parameters from a set of CBCT projections of calibration phantom by traversing it around the rotation axis. The internal parameters represent the structure of image subsystem. The external parameters represent the orientation and position of calibration phantom in image subsystem. DLT method in camera calibration technique was applied here. The details are demonstrated in reference [5].

(2) The two parts, which need to be changed, were calculated based on the parameters obtained in step (1). The details are demonstrated in *B.1* and *B.2*.

(3) The improved FDK algorithm was applied to obtain the sectional images from a set of CBCT projections of object by traversing it around the rotation axis.

#### B.1. Calculation of voxel projection on misaligned detector

As shown in Figure 1, the process of voxel projection on the detector in CBCT system is similar to camera imaging. The formula to describe the process of CBCT projection is as follows:

$$s\begin{bmatrix}u\\v\\1\end{bmatrix}=\begin{bmatrix}f/dx & 0 & u_0 & 0\\0 & f/dy & v_0 & 0\\0 & 0 & 1 & 0\end{bmatrix}\begin{bmatrix}r & t\\0^T & 1\end{bmatrix}\begin{bmatrix}cos\theta & -sin\theta & 0 & 0\\sin\theta & cos\theta & 0 & 0\\0 & 0 & 1 & 0\\0 & 0 & 0 & 1\end{bmatrix}\begin{bmatrix}X\\Y\\Z\\1\end{bmatrix} \quad (1)$$

Equation (1) can be rewritten as:

$$sC_{projection} = A \cdot R \cdot R(\theta) \cdot C_{voxel} \quad (2)$$

In equation (2), $C_{voxel}$ represents the voxel coordinate in initial position defined in rotation subsystem, $R(\theta)$ represents the rotation matrix of a certain angle $\theta$ around the rotation axis, $R$ represents the external matrix which is the transformation from rotation subsystem to image subsystem, $A$ represents the internal matrix which represents the transformation from image subsystem to 2D image coordinates, $C_{projection}$ represents the projection coordinate of voxel on detector no matter it is ideal or misaligned. $A$ and $R$ are unknown parameters in equation (2). The details of $A$ and $R$ calculation are as follows.

Matrix $A$ was calculated as follows. Firstly, $A$ was directly calculated in every position of traversed calibration phantom using DLT method. Then, the mean values of internal matrices in different positions were obtained to reduce the random noise.

Matrix $R$ represents the misalignments. The correction can be done by introduce $R$ into the imaging formula, like equation (2). As shown in Figure 1, to describe the external matrix in CBCT system, two right-handed Cartesian coordinate systems are introduced: image coordinate system and rotation coordinate system. Origin of image coordinate system is the X-ray source, which is denoted by $O^I$. $Z^I$ axis is the optical axis. $X^I$, $Y^I$ axes are parallel to the $u$ and $v$ axes of detector respectively. Origin of rotation coordinate system is the foot point of source on $Z^R$ axis, which is denoted by $O^R$. $Z^R$ axis is the rotation axis. $X^R$ axis is the line connecting source and $O^R$.

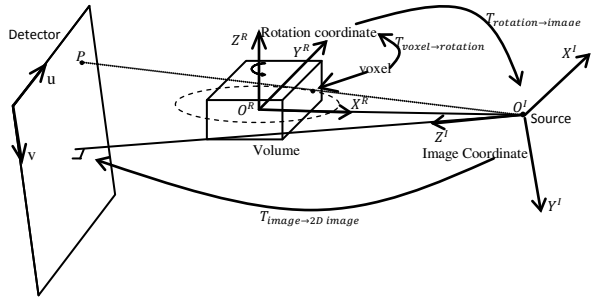


Figure1. Coordinate systems in misaligned CBCT. The voxel traverses around the rotation axis $Z^R$, along a circular trajectory represented as the dashed line. Projections of the object were collected during the process. The voxel and volume are defined in rotation coordinate. The point $P$ is the projection of voxel on the misaligned detector. $T_{voxel\rightarrow rotation}$, $T_{rotation\rightarrow image}$, $T_{image\rightarrow 2D\ image}$ respectively represent $R(\theta)$, $R$, $A$ in equation (2).

To calculate matrix $R$ in CBCT system, the vectors of rotation coordinate axes in both image and rotation coordinate should be obtained. Firstly, the vector of rotation axis in image coordinate was calculated as follows. In image coordinate system, locations of calibration phantom origin can be represented by the vectors $t_j$ in matrix $\begin{bmatrix}r_j & t_j\\0^T & 1\end{bmatrix}$, which can be directly obtained by DLT method. The locations of traversed calibration phantom can form a circular trajectory with circle center on the rotation axis. Assuming $n$ projections are acquired, the circle center $C^I$ is the mean value of the locations:

$$C^I = \frac{1}{n}\sum_{j=1}^{n} t_j \quad (3)$$

The vector of rotation axis in image coordinate, which was denoted by $Z^{RI}$, was calculated as follows. Rotation axis is the normal vector of the plane formed by the traversed calibration phantom trajectory. $Z^{RI}$ is as follows:

$$Z^{RI} = \frac{1}{n}\sum_{j=1}^{n}\left(t_{j+k} - t_j\right) \times \left(t_{j+l} - t_{j+k}\right) \quad (4)$$

In equation (4), $k = \left\lfloor \frac{1}{3}n \right\rfloor$, $l = \left\lfloor \frac{2}{3}n \right\rfloor$, $j + k = mod((j+k), n), j + l = mod((j+l), n)$.

The vector of rotation coordinate origin $O^R$ in image coordinate, which was denoted by $O^{RI}$, was calculated as follows. Rotation coordinate origin is the foot point of source $O^I$ on the rotation axis $Z^{RI}$. Given one point $C^I$ on $Z^{RI}$ and coordinate of $O^I$, which is $(0,0,0)^T$, $O^{RI}$ is as follows:

$$O^{RI} = C^I - \frac{((O^I - C^I), Z^{RI})}{\|Z^{RI}\|^2} \cdot Z^{RI} \quad (5)$$

The vector of $X^R$ axis in image coordinate, which was denoted by $X^{RI}$, was calculated as follows. $X^R$ axis is the line connecting source $O^I$ and $O^R$. $X^{RI}$ is as follows:

$$X^{RI} = O^I - O^{RI} \quad (6)$$

The vector of $Y^R$ axis in image coordinate, which was denoted by $Y^{RI}$, was calculated as follows. $Y^R$ axis is the cross product of $Z^{RI}$ and $X^{RI}$. $Y^{RI}$ is as follows:

$$Y^{RI} = Z^{RI} \times X^{RI} \quad (7)$$

Based on equations (4-7), the unit vectors of rotation coordinate axes in image coordinate are calculated as:

$$V^R = [O^{RI}, X^{RI}/\|X^{RI}\|, Y^{RI}/\|Y^{RI}\|, Z^{RI}/\|Z^{RI}\|] \quad (8)$$

The unit vectors of rotation coordinate axes in rotation coordinate are denoted as:

$$V^I = \begin{bmatrix}0 & 1 & 0 & 0\\0 & 0 & 1 & 0\\0 & 0 & 0 & 1\\1 & 1 & 1 & 1\end{bmatrix} \quad (9)$$

The external matrix $R$ can be calculated as:

$$R = V^I \cdot (V^R)^{-1} \quad (10)$$

Based on equations (2-10), the projection coordinate of reconstructed voxel on misaligned detector at certain rotating angle $\theta$ can be calculated.

### *B.2. Calculation of weighting factor*

As for our improved FDK algorithm, the weighting factor based on the reconstructed voxel should also be changed. The calculation of the weighting factor is as follows.

$$w = \frac{{D_S}^2}{(D_S - x^*)^2} \quad (11)$$

In equation (11), $D_S$ represents the distance between $O^I$ and $O^R$, that is, the length of $X^{RI}$:

$$D_S = \|X^{RI}\| \quad (12)$$

In equation (11), $x^*$ represents the coordinate of voxel after rotating by a certain angle $\theta$. The calculation of $x^*$ is as follows:

$$x^* = x_{voxel} \cdot cos\theta + y_{voxel} \cdot sin\theta \quad (13)$$

## III. Simulation and Results

Simulations were conducted to verify the performance of the improved FDK algorithm. Firstly, DLT was applied to calibrate the parameters using calibration phantom with 12 markers. The parameters include matrix $A$, matrix $R$ and $D_S$. Secondly, the CBCT projections of thin-walled sphere phantom were obtained both in ideal and misaligned CBCT systems. Thirdly, three different types of results were obtained: (1) reconstructed result of projections in ideal CBCT system with standard FDK algorithm, (2) reconstructed result of projections in misaligned CBCT system with improved FDK algorithm, (3) reconstructed result of projections in misaligned CBCT system with standard FDK algorithm. The simulation parameters are as follows.

The parameters of calibration phantom used in DLT method are as follows.

TABLE I. Coordinates of Markers in Calibration Phantom

| I | C | I | C | I | C | I | C |
|---|---|---|---|---|---|---|---|
| 1 | (5.0,-8.0,8.0) | 4 | (0.0,-8.0,0.0) | 7 | (5.0,-8.0,-5.0) | 10 | (0.0,-8.0,-8.0) |
| 2 | (5.0,0.0,8.0) | 5 | (0.0,0.0,0.0) | 8 | (5.0,0.0,-5.0) | 11 | (0.0,0.0,-8.0) |
| 3 | (5.0,8.0,8.0) | 6 | (0.0,8.0,0.0) | 9 | (5.0,8.0,-5.0) | 12 | (0.0,8.0,-8.0) |

(The unit is 'mm'; 'I' represents markers index, 'C' represents coordinates)

Here we acquired 360 projections of the calibration phantom. The angular interval of the rotating was 1°.

The parameters of the thin-walled sphere are as follows.

TABLE II. Parameters of Thin-walled Sphere

| Center coordinates(mm) | half axis(mm) | CT Value |
|---|---|---|
| (0,0,0) | (15.0,15.0,15.0) | 1.0 |
| (0,0,0) | (14.8,14.8,14.8) | -0.9 |

The parameters of the system geometry are as follows:

(1) Detector array was 1024×1024 with pixel size of 50μm

(2) The distance from X-ray source to the rotation axis was 200mm.

(3) The distance from X-ray source to the detector was 220mm.

(4) The size of reconstruction matrix was 384×384×384

(5) The size of voxel was $0.1\times0.1\times0.1mm^3$

(6) The interval of projection was 1° within 0-360°

In this paper, firstly, yaw, pitch or roll misalignment of detector, which represent rotations along central row, central column and the detector center respectively, were simulated. Then, combined misalignment of detector was simulated. The reconstruction results are as follows.

(1)Detector with yaw misalignment of $10^{\circ}$:

The calculated parameters are as follows:

$$A = \begin{bmatrix} 4333 & 0 & 512 & 0 \\ 0 & 4333 & -252 & 0 \\ 0 & 0 & 1 & 0 \end{bmatrix}$$

$$R = \begin{bmatrix} 1 & 0 & 0 & 0 \\ 0 & 0.98 & 0.17 & 34.7 \\ 0 & -0.17 & 0.98 & 196.9 \\ 0 & 0 & 0 & 1 \end{bmatrix}, D_S = 200.02$$

The reconstruction results are as follows:

(a1) (a2) (a3)

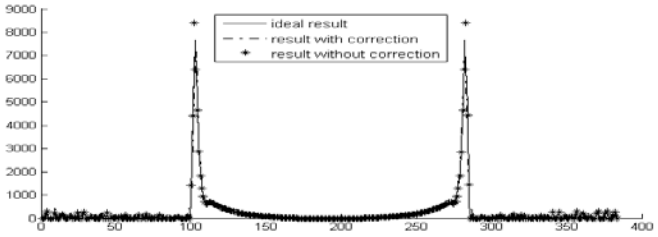


(a4)

Figure2. Reconstruction results of simulated projections when yaw misalignment exists. (a1) Ideal result of 100th layer. (a2) Result of 100th layer with improved FDK algorithm. (a3) Result of 100th layer with standard FDK algorithm. (a4) Difference between ideal result, result with correction and result without correction.

(2) Detector with pitch misalignment of $10^{\circ}$:

The calculated parameters are as follows:

$$A = \begin{bmatrix} 4333 & 0 & -251 & 0 \\ 0 & 4333 & 513 & 0 \\ 0 & 0 & 1 & 0 \end{bmatrix},$$

$$R = \begin{bmatrix} 0.98 & 0 & 0.17 & 34.7 \\ 0 & 1 & 0 & 0 \\ -0.17 & 0 & 0.98 & 196.9 \\ 0 & 0 & 0 & 1 \end{bmatrix}, D_S = 200.00$$

The reconstruction results are as follows:

(b1) (b2) (b3)

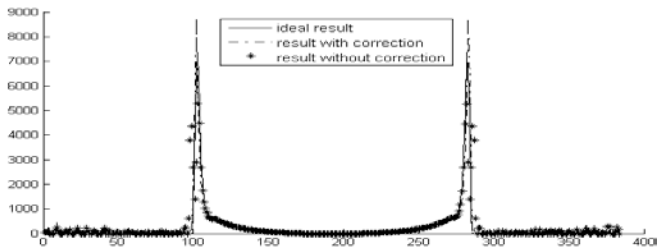


(b4)

Figure3. Reconstruction results of simulated projections when pitch misalignment exists. (b1) Ideal result of 100th layer. (b2) Result of 100th layer with improved FDK algorithm. (b3) Result of 100th layer with standard FDK algorithm. (b4) Difference between ideal result, result with correction and result without correction.

(3) Detector with roll misalignment of $10^{\circ}$:

The calculated parameters are as follows:

$$A = \begin{bmatrix} 4400 & 0 & 512 & 0 \\ 0 & 4400 & 513 & 0 \\ 0 & 0 & 1 & 0 \end{bmatrix}$$

$$R = \begin{bmatrix} 0.98 & -0.17 & 0 & 0 \\ 0.17 & 0.98 & 0 & 0 \\ 0 & 0 & 1 & 200.0 \\ 0 & 0 & 0 & 1 \end{bmatrix}, D_S = 200.00$$

The reconstruction results are as follows:

(c1) (c2) (c3)

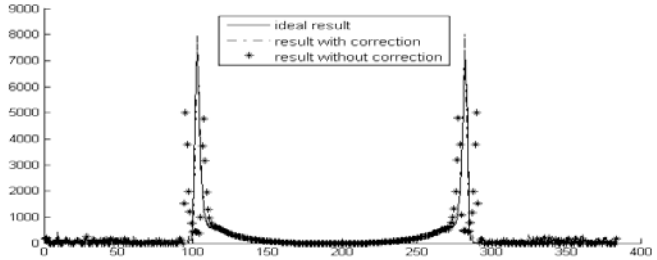


(c4)

Figure4. Reconstruction results of simulated projections when roll misalignment exists. (c1) Ideal result of 100th layer. (c2) Result of 100th layer with improved FDK algorithm. (c3) Result of 100th layer with standard FDK algorithm. (c4) Difference between ideal result, result with correction and result without correction.

(4) Detector with combined misalignments: roll angle of $10^{\circ}$, pitch angle of $10^{\circ}$, yaw angle of $10^{\circ}$.

The calculated parameters are as follows:

$$A = \begin{bmatrix} 4267 & 0 & -96 & 0 \\ 0 & 4267 & -370 & 0 \\ 0 & 0 & 1 & 0 \end{bmatrix},$$

$$R = \begin{bmatrix} 0.96 & -0.20 & 0.13 & 27.7 \\ 0.17 & 0.96 & 0.20 & 40.1 \\ -0.17 & -0.17 & 0.96 & 193.9 \\ 0 & 0 & 0 & 1 \end{bmatrix}, D_S = 199.97$$

The reconstruction results are as follows:

(d1) (d2) (d3)

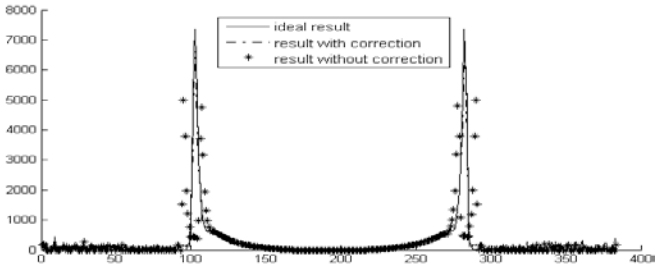


(d4)

Figure5. Reconstruction results of simulated projections when combined misalignments exist. (d1) Ideal result of 100th layer. (d2) Result of 100th layer with improved FDK algorithm. (d3) Result of 100th layer with standard FDK algorithm. (d4) Difference between ideal result, result with correction and result without correction.

## IV. Discussion and Conclusion

As for the simulation, we simulated the detector misalignments of $10^{\circ}$, which is suitable to observe the artifacts and to verify the efficiency of our improved FDK algorithm. Besides, we also simulated slighter misalignments of $2^{\circ}$. The results, which are not demonstrated for the lack of space, also verified the efficiency of our improved algorithm.

From figure 2-4, we can see that the pitch and roll misalignments of detector will cause more severe artifacts than yaw misalignment. This shows that CBCT is less sensitive for detector vertical error than detector horizontal error. Figure 2-5 show that the improved FDK algorithm reduced the artifacts significantly compared with standard FDK algorithm in misaligned CBCT. We can draw a conclusion that this improved FDK algorithm can reconstruct misaligned CBCT sectional image efficiently.

In this paper, an improved FDK algorithm using camera calibration technique for misaligned CBCT reconstruction is presented. Camera calibration technique is easy to implement with a reliable performance, which ensures the efficiency of the method in this paper. Our lab developed a micro-CBCT system recently. The future work will be focused on applying the algorithm on real system.

## References


[1] Marek Karolczak, Stefan Schaller, et al., "Implementation of cone-beam reconstruction algorithm for the single-circle source orbit with embedded misalignment correction using homogeneous coordinates", Medical Physics, 2001, Vol. 28(10), pp. 2050-2069

[2] Yi Sun, Ying Hou, and Jiasheng Hu, "Reduction of artifacts induced by misaligned geometry in cone-beam CT", *IEEE Transaction on Biomedical Engineering*, 2007, Vol. 54, No. 8, pp. 1461-1471

[3] Ramesh R. Galigekere, Karl Wiesent, and David W. Holdsworth, "Cone-beam Reprojection Using Projection-matrices", IEEE transaction on medical imaging. 2003, Vol. 22, No. 10, pp. 1202-1214

[4] L. A. Feldkamp, L. C. Davis, and J. W. Kress, "Practical cone-beam algorithm", *J. Opt. Soc. Am. A.,* 1984, vol. 1, no. 6, pp.612-619

[5] Y. I. Abdel-Aziz, H. M. Karara. "Direct linear transformation into object space coordinates in close-range photogrammetry", Univ. of Illinois at Urbana Champaign, Urbana, 1971, pp. 1-18